Journal of Engineering and Natural Sciences
Mühendislik ve Fen Bilimleri Dergisi

Sigma 33, 188-199, 2015

Research Article / Araştırma Makalesi

RESONANT VIBRATIONS OF TWO-SPAN RAILWAY BRIDGES UNDER HIGH-SPEED TRAINS

Volkan KAHYA*[1], Onur ARAZ[2], Muhittin TURAN[1]

[1] *Karadeniz Technical University, Faculty of Engineering, Department of Civil Engineering, TRABZON*
[2] *Gümüşhane University, Department of Civil Engineering, GÜMÜŞHANE*

Received/Geliş: 25.01.2015 Revised/Düzeltme: 04.05.2015 Accepted/Kabul: 18.05.2015

ABSTRACT

In this study, resonant vibrations of two-span railway bridges subjected to high-speed trains (HSTs) are studied. The continuous beam is modelled by using Bernoulli-Euler beam theory, and the train is considered as a series of moving concentrated loads. The dynamic response is obtained analytically by using the assumed mode method. Effects of the speed parameter and the span to car length ratio on the response are examined. Numerical results show that the above mentioned parameters play very important role on the dynamic behavior of two-span bridges.
Keywords: Continuous bridge, high-speed train, resonant vibration, moving load, railway bridge.

İKİ AÇIKLIKLI DEMİRYOLU KÖPRÜLERİNİN HIZLI TREN GEÇİŞLERİ ALTINDAKİ REZONANS TİTREŞİMLERİ

ÖZET

Bu çalışmada iki açıklıklı demiryolu köprülerinin hızlı tren geçişleri altındaki rezonans titreşimleri ele alınmıştır. Sürekli kiriş, Euler-Bernoulli teorisine göre modellenmiş, tren ise tekil yüklerden oluşan bir yük katarı şeklinde düşünülmüştür. Mod birleştirme metodu kullanılarak dinamik tepkiler analitik olarak elde edilmiştir. Hız parametresi ve açıklık / vagon uzunluğu oranının dinamik davranış üzerindeki etkileri incelenmiştir. Sayısal sonuçlar, bahsedilen bu parametrelerin iki açıklıklı köprülerin dinamik davranışını önemli ölçüde etkilediğini göstermektedir.
Anahtar Sözcükler: Sürekli kiriş, yüksek hızlı tren, rezonans titreşimi, hareketli yük, demiryolu köprüsü.

---

1. INTRODUCTION

The dynamic response of railway bridges under trains moving at resonant speeds is of great importance. Many researchers have contributed to the solution of the problem with their improvements, and still the dynamics of bridges under high-speed trains (HSTs) is a subject that draws considerable attention of researchers. Moving load induced intensive vibrations on the bridge are not desired because they significantly affect the transportation safety. When a train travels over a bridge at a resonant speed, the response of the bridge tends to increase steadily as there are more loads passing the bridge [1, 2]. This is the so-called "resonance phenomenon", and

* Corresponding Author/Sorumlu Yazar: e-mail/e-ileti: volkan@ktu.edu.tr, tel: (462) 377 26 31

it can cause passenger discomfort, a reduction of the service life of the bridge, ballast deconsolidation, and subsequent risk of derailment [3].

A numerous studies related to the moving load problems for simply supported beams have been reported in the literature [4-7]. For continuous beams, the vibration of a beam with two equal spans under a constant moving force was first solved by Ayre *et al.* [8]. Henchi and Fafard [9] used an exact dynamic stiffness element in the finite element approximation to study the dynamic response of multi-span structures under a convoy of moving loads. They developed a dynamic model coupled with a fast Fourier transform (FFT) algorithm. Ichikawa *et al.* [10] investigated the dynamic response of a multi-span Euler-Bernoulli beam subjected to a moving load with time-dependent velocity using the modal analysis. They estimated the effects of acceleration or deceleration of the moving load on the dynamic amplification factor for a symmetric three-span continuous beam. Kwark *et al.* [11] studied dynamic response of two-span continuous concrete bridges under the Korean HST by employing the experimental and theoretical methods. Martinez-Castro *et al.* [12] presented a semi-analytical solution for damped non-uniform continuous beams. They modeled the moving loads by the Dirac Delta function, and the modal loads were obtained in terms of cubic Hermitian polynomials. Johansson *et al.* [13] derived a closed-form solution for evaluating the dynamic behavior of a general multi-span Bernoulli-Euler beam. The natural frequencies of vibration and corresponding mode shapes were obtained by applying the boundary conditions to the characteristic function of the beam.

Although above-mentioned studies gave some results on moving load-induced vibrations of single or multi-span beams, no further details were presented for the resonant vibrations of two-span continuous beams. In the present study, the dynamic response of two-span bridges under HSTs is investigated with an emphasis on the resonant vibration. The impact factors (*I*) for dynamic reactions at different sections of each span are calculated depending on the speed parameter and the span to car length ratio.

2. MATHEMATICAL FORMULATION

Fig. 1 shows a two-span continuous beam with equal span length *L* and uniform cross section subjected to a series of moving loads at a constant speed *v*. Neglecting the damping of the beam, the governing equation of motion can be written as

$$EI\frac{\partial^4 y(x,t)}{\partial x^4}+m\frac{\partial y^2(x,t)}{\partial t^2}=F(x,t) \tag{1}$$

where *m* is the mass per unit length, $y=y(x,t)$ is the transverse displacement of any beam section at time *t*, *x* refers to the longitudinal coordinate, and *EI* is the flexural stiffness of beam. $F(x,t)$ is the loading function and can be defined as

$$F(x,t)=\sum_{k=1}^{N}P_k\delta(x-x_k)\left[H(t-t_k)-H(t-t_k-\frac{2L}{v})\right] \tag{2}$$

where $x_k=vt-d_k$ the distance of the *k*th load to the left-end of the beam, d_k is the distance of *k*th load to the first one ($d_1=0$), *N* is the total number loads, P_k is the magnitude of the *k*th load, $t_k=d_k/v$ entrance time of the *k*th load to the beam, $\delta(\bullet)$ is the Dirac delta function, and $H(\bullet)$ is the Heaviside function.

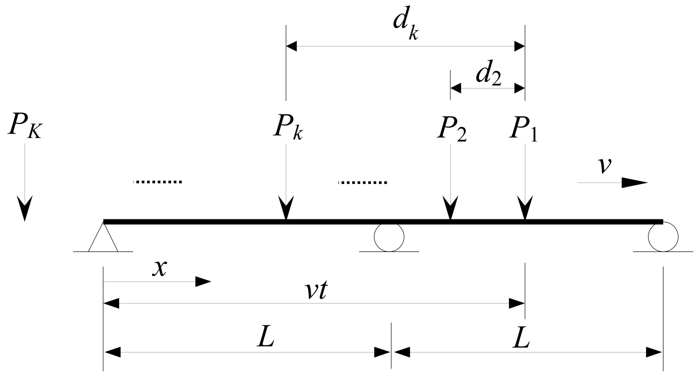

Figure 1. A two-span continuous beam subjected to a series of moving loads

In solution, the assumed mode method is employed. Thus, the displacement of the beam can be expressed as

$$y(x,t)=\sum_{n=1}^{\infty}\phi_n(x)Y_n(t) \quad n=1,2,\cdots,\infty \tag{3}$$

where $Y_n(t)$ is the generalized coordinates associated with the *n*th natural mode and $\phi_n(x)$ is the *n*th modal shape function of the beam.

Substituting Eqs. (2) and (3) into Eq. (1), multiplying both sides of the resulting expression by $\phi_m(x)$, and integrating the result with respect to *x* between 0 and 2*L*, the equation of motion in terms of the generalized displacement $Y_n(t)$ can be obtained as the follows with considering the orthogonality conditions of the modes.

$$\sum_{n=1}^{\infty}\ddot{Y}_n+\omega_n^{\,2}\sum_{n=1}^{\infty}Y_n=\frac{2P}{mL}\sum_{k=1}^{K}\phi_n(x_k)\left[H(t-t_k)-H(t-t_k-\frac{2L}{v})\right] \tag{4}$$

where over dot indicates differentiation with respect to time and ω_n represents *n*th circular natural frequency of the two-span bridge. If first *N* modes of vibration are considered, Eq. (4) constitutes *N* equations for *N* unknowns. The solution can be obtained easily by using the Newmark's method with $\beta=1/4$ and $\gamma=1/2$ [15].

3. MODAL SHAPE FUNCTIONS OF TWO-SPAN CONTINUOUS BEAMS

The modal shape functions of two-span continuous beams can be divided into two groups: symmetric and antisymmetric. The circular natural frequency for symmetric and antisymmetric modes can be expressed as

$$\omega_n=\frac{\beta_n^2}{L^2}\sqrt{\frac{EI_b}{m}},\quad \beta_n^2=\begin{cases}\left(\dfrac{n+1}{2}\pi\right)^2 & n=1,3,5,\ldots\\[2mm] \left(\dfrac{2n+1}{4}\pi\right)^2 & n=2,4,6,\ldots\end{cases} \tag{5}$$

Then, the modal shape functions can be expressed as

$$\phi_n(x_1) = \left[\sin\beta_n x_1 - \frac{\sin\beta_n L}{\sinh\beta_n L}\sinh\beta_n x_1 \right] \; x_1 \in [0, L],$$

$$\phi_n(x_2) = -\left[\sin\beta_n x_2 - \frac{\sin\beta_n L}{\sinh\beta_n L}\sinh\beta_n x_2 \right] \; x_2 \in [2L, L] \quad n = 1,3,5,\ldots \tag{6}$$

$$\phi_n(x_1) = \left[\sin\beta_n x_1 - \frac{\sin\beta_n L}{\sinh\beta_n L}\sinh\beta_n x_1 \right] \; x_1 \in [0, L],$$

$$\phi_n(x_2) = \left[\sin\beta_n x_2 - \frac{\sin\beta_n L}{\sinh\beta_n L}\sinh\beta_n x_2 \right] \; x_2 \in [2L, L] \quad n = 2,4,6,\ldots \tag{7}$$

4. RESONANCE SPEEDS

As it well known, resonance in the bridge may occur by depending on the train type, *i.e.*, the distance between its axles, in a speed as [1, 4, 6]:

$$\frac{\pi v_{n,i}}{\omega_n L} = \frac{d}{2iL} \quad \text{or} \quad v_{n,i} = \frac{\omega_n d}{2\pi i} \quad n = 1,2,\ldots, i = 1,2,\ldots, \tag{8}$$

where ω_n, L and d are nth the natural circular frequency of the beam, span length and the characteristic distance between the train loads, which is generally assumed as the car length, respectively. For simplicity, we shall introduce the following dimensionless variable:

$$S = \frac{v}{v_{cr}} = \frac{v}{v_{2,1}} \tag{9}$$

where, S is the dimensionless speed parameter, v_{cr} is the critical speed or the 1st resonance of 2nd mode vibration, and v is the train speed. By letting i = 1,2,3,..., the preceding equation indicates that resonance may occur at the following dimensionless speeds: S = 1, 0.5, 0.333,... for n = 2, and S = 0.64, 0.32, 0.213,... for n = 1 with diminishing values. Fig. 2 gives train speed – span to car length ratio curves for different dimensionless speeds calculated by Eqs. (8) and (9). As seen in the figure, since todays HSTs can reach the speeds within 250-350km/h, speeds for the 1st resonance of 2nd vibration mode (S = 1) are not possible considering today's technology, but speeds for S = 0.64, 0.5 and 0.32 are possible for different span to car length ratio.

5. NUMERICAL RESULTS

For the purpose of illustration, a number of two span bridges made of pre-stressed concrete with E = 29.43 GPa and having different span lengths L are considered. It is assumed that the mass per unit length and the frequency of vibration of each bridge are defined as follows: $m = 30 + 0.2L$ t/m and $\omega_1 = 900/L$ rad/s [4]. In order to study the effect of span to car length ratio (L/d) on the bridge dynamic response, 16 values for L/d within 0.5 – 2 are considered. Speed parameter (S) is considered between 0.0 – 1.0. The increment in S for each dynamic analysis is selected as 0.01, and for each L/d, the results are, thus, obtained for 100 different train speeds in the dynamic analysis. Eurostar, a European HST, is selected as a moving vehicle and is simplified as a series of moving concentrated forces as shown in Fig. 3. For this vehicle, characteristic car length (d) is 18.7m.

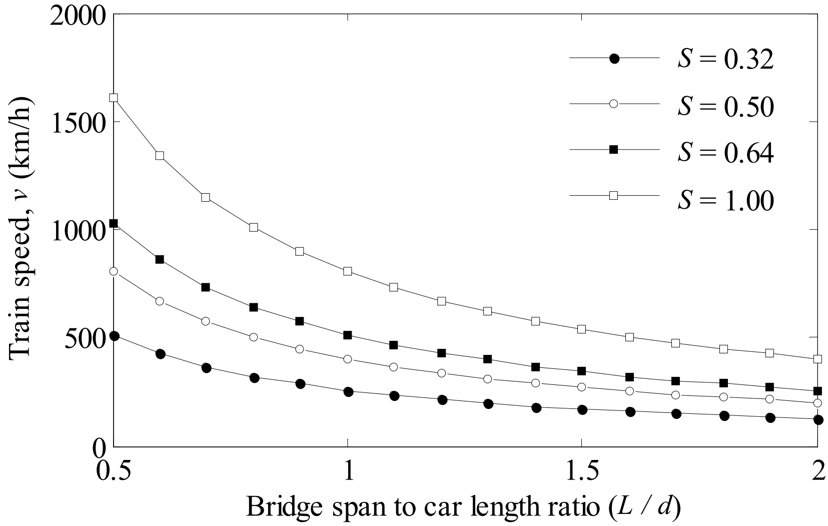

Figure 2. Train speed *vs.* L / d plot for different dimensionless speeds

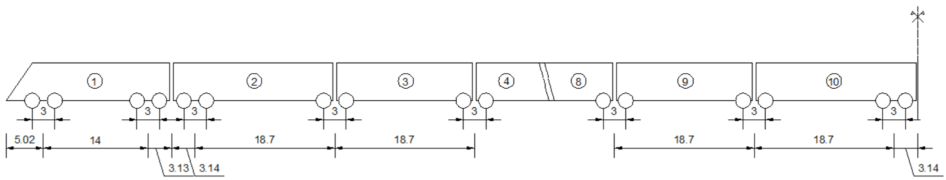

Figure 3. Eurostar HST configuration (units in m)

In the following, graphs are given for the impact factor of any response parameter. The impact factor (I) is defined as [4, 14]:

$$I = \frac{D_{dyn} - D_{sta}}{D_{sta}} \tag{10}$$

where D_{dyn} and D_{sta} denote, respectively, the maximum dynamic and static response of the bridge at a section x due to the passage of moving load.

The impact factors I_D computed for the dynamic vertical displacement at the middle of each span are plotted with respect to the speed parameter S and the span to car length ratio L/d in Figs. 4 and 5 along with contour lines. An important trend revealed by these figures is that the shorter the span length of a two span bridge, the larger the impact factor for the displacement of the each span. Another observation from the figures is that the dynamic responses for the resonance points with S = 1.0, 0.64 and 0.5 are of practical significance, while the other resonant responses can generally be neglected in practice. Considerable is the fact that when $L/d = 1.5$, nearly no resonant response will be induced on the bridge due to the passage of trains, as can be seen in the contour lines in Figs. 3 and 4. Another merit with the figures is that the impact factor for the second span is slightly larger than that of the first. Finally, we can also observe that if the operation speeds of the train can be controlled in the range with $0.0 \leq S < 0.4$ the minimal resonant responses will be induced on the bridge.

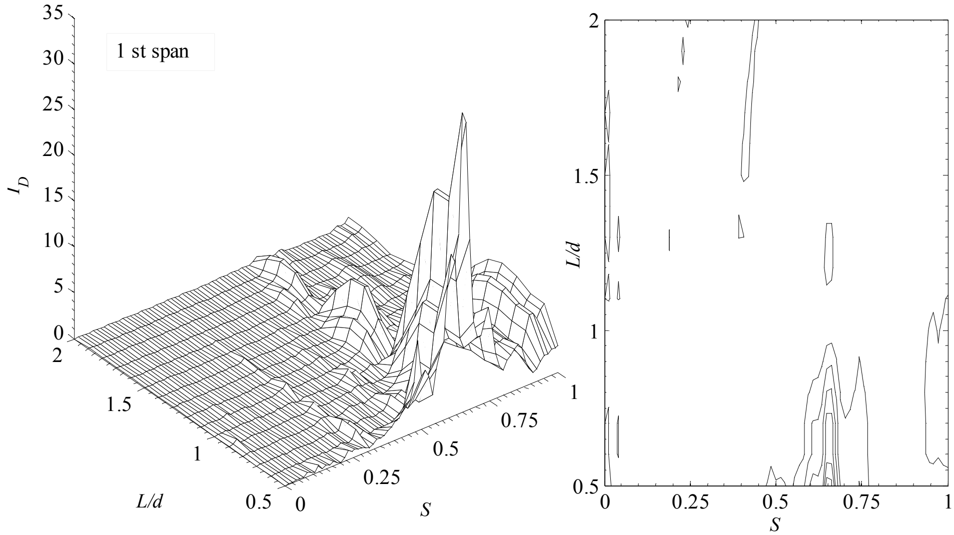

Figure 4. Effect of the span to car length ratio on the impact factor for displacement at the middle of first span: $I - S - L/d$ diagram and contour lines

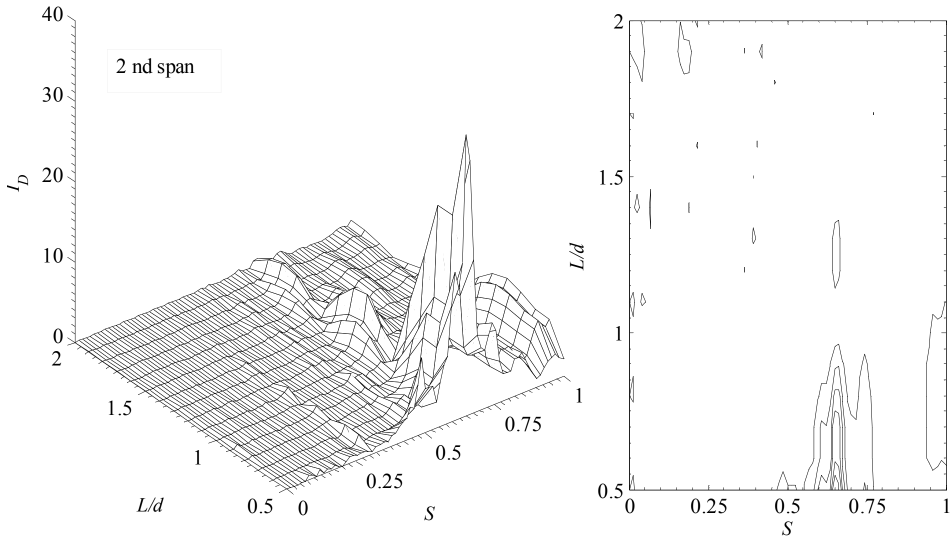

Figure 5. Effect of the span to car length ratio on the impact factor for displacement at the middle of second span $I - S - L/d$ diagram and contour lines

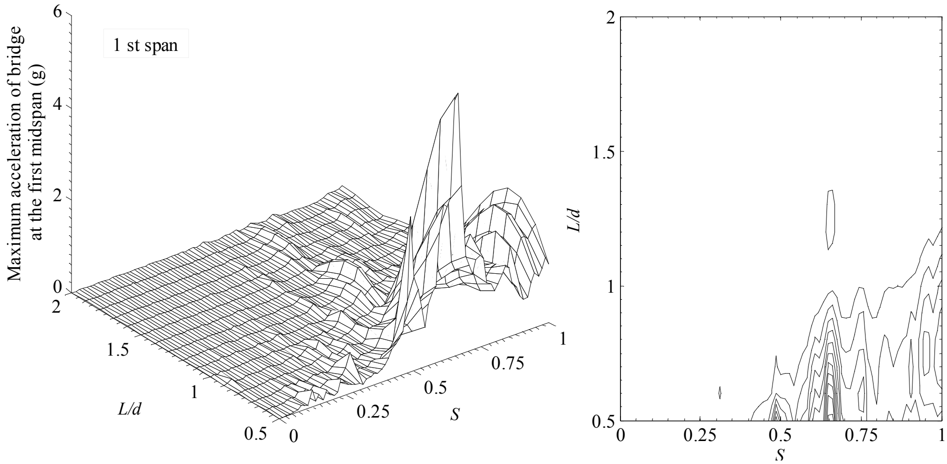

Figure 6. Effect of the span to car length ratio on the maximum acceleration at the middle of first span: $a - S - L/d$ diagram and contour lines

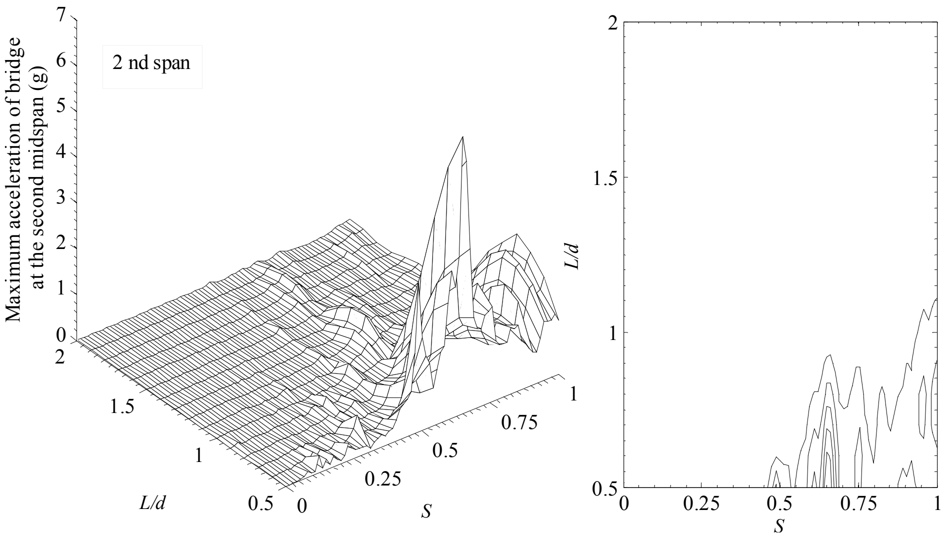

Figure 7. Effect of the span to car length ratio on the maximum acceleration at the middle of second span: $a - S - L/d$ diagram and contour lines.

Figs. 6 and 7 along with contour lines show maximum accelerations computed at the middle of each span with respect to the speed parameter *S* and the span to car length ratio L/d. One can make similar observations from these figures as in Figs. 4 and 5.

Figs. 8-10 along with contour lines give the impact factors I_M for the bending moment at the middle of each span and the second support of the bridge with respect to the speed parameter *S* and the span to car length ratio L/d. As can be seen, the impact factor I_M for bending moment at the second support of the bridge is smaller than those for bending moments at the middle of first and second spans.

The impact factors I_S for the shear force at both ends of each span are plotted with respect to the speed parameter *S* and the span to car length ratio L/d in Figs. 11-14 along with contour lines. The impact factors for shear force (I_S) at the right-ends of each span are smaller than those at the left-ends. Another observation from the figures is that the dynamic shear force and bending moment for the resonance points with S = 1.0, 0.64 and 0.5 are of practical significance, while the other resonant responses can generally be neglected in practice.

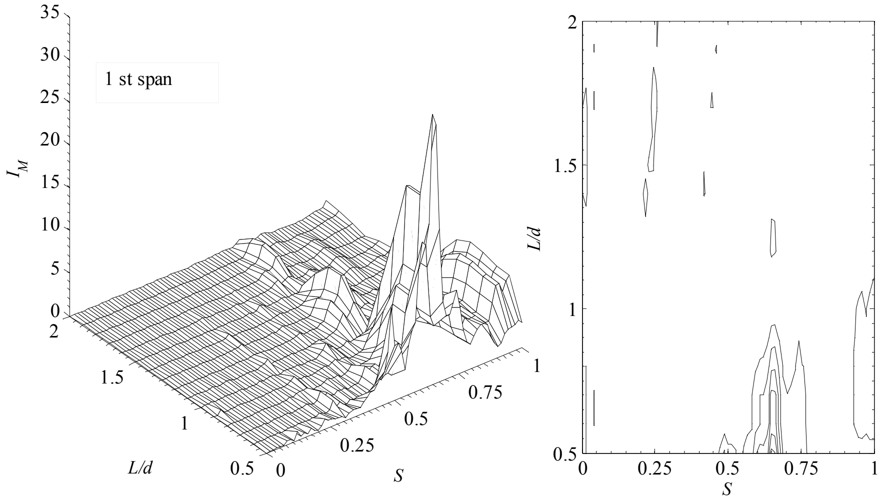

Figure 8. Effect of the span to car length ratio on the impact factor for bending moment at the middle of first span: $I-S-L/d$ diagram and contour lines

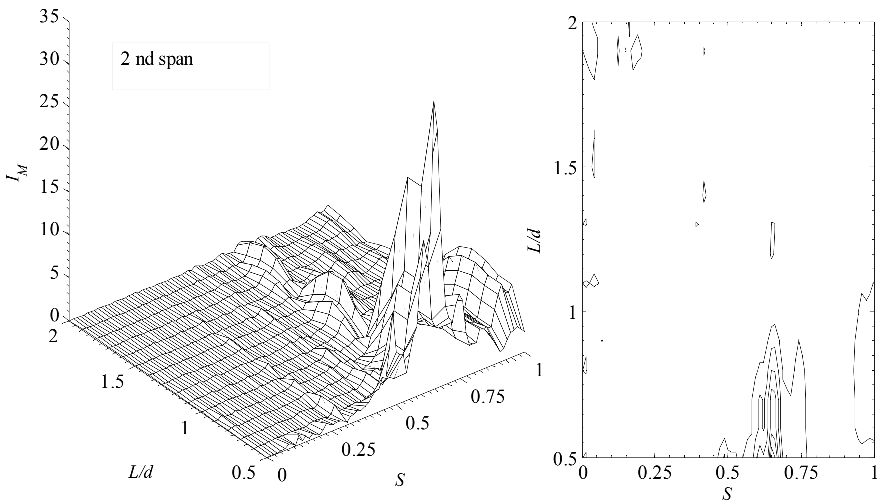

Figure 9. Effect of the span to car length ratio on the impact factor for bending moment at the middle of second span: $I-S-L/d$ diagram and contour lines

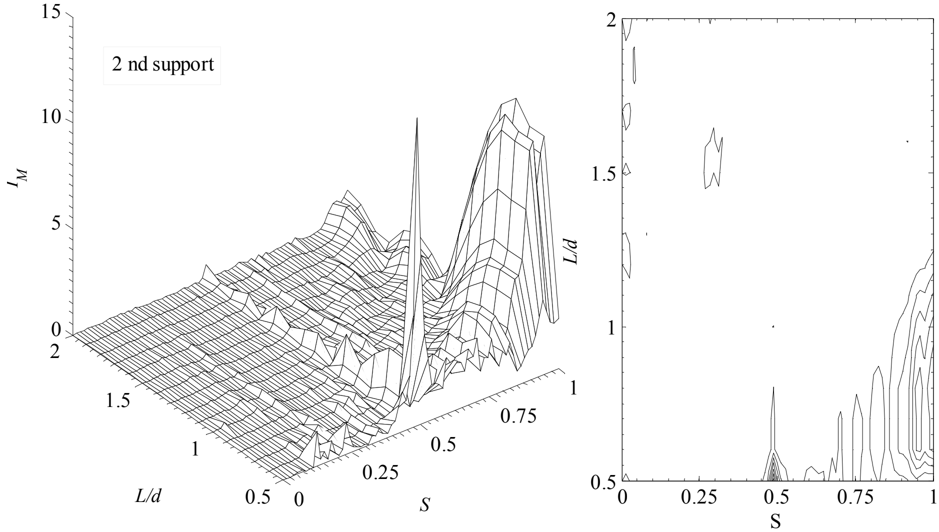

Figure 10. Effect of the span to car length ratio on the impact factor for bending moment at the middle support of the bridge: $I-S-L/d$ diagram and contour lines

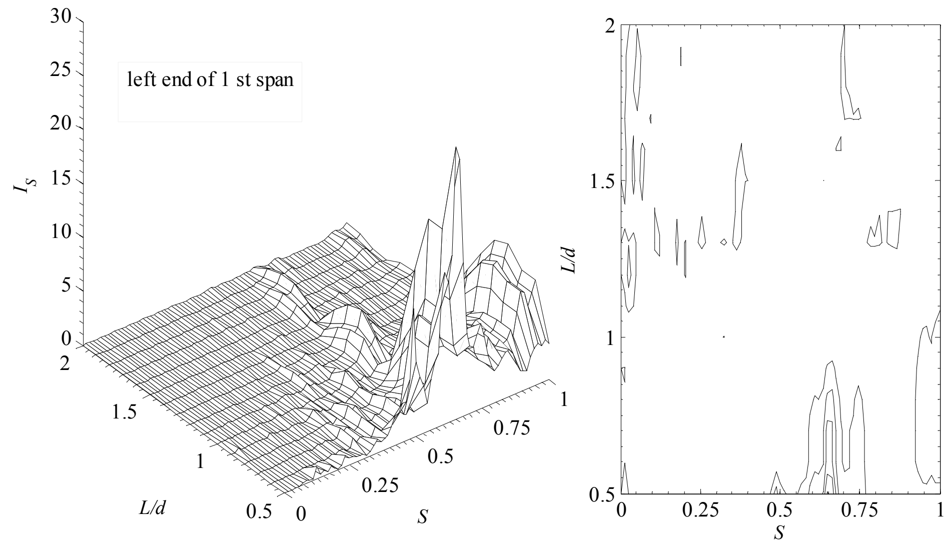

Figure 11. Effect of the span to car length ratio on the impact factor for shear force at the left-end of first span: $I-S-L/d$ diagram and contour lines

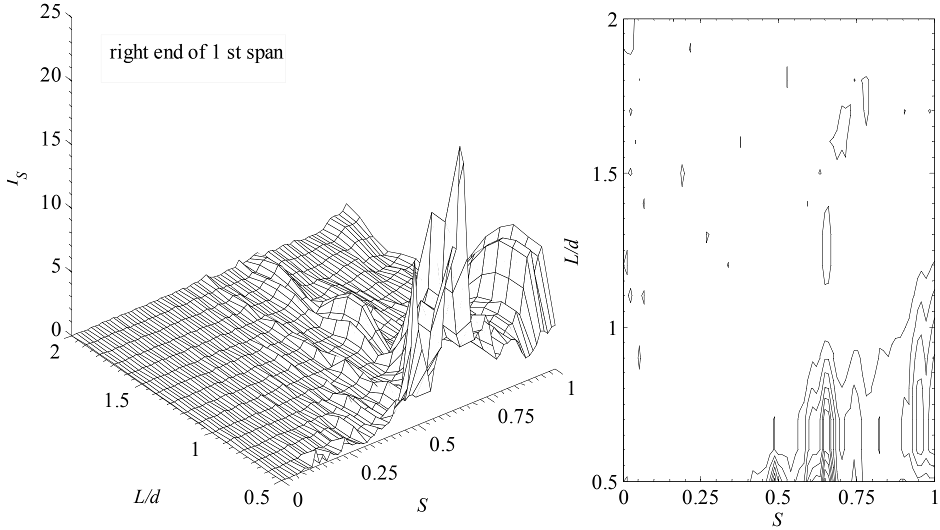

Figure 12. Effect of the span to car length ratio on the impact factor for shear force at the right-end of first span: $I-S-L/d$ diagram and contour lines

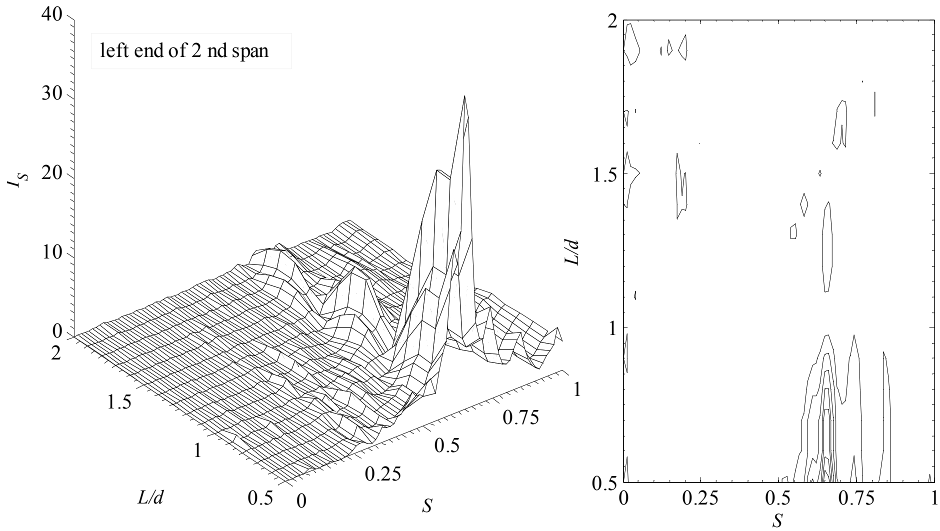

Figure 13. Effect of the span to car length ratio on the impact factor for shear force at the left-end of second span: $I-S-L/d$ diagram and contour lines

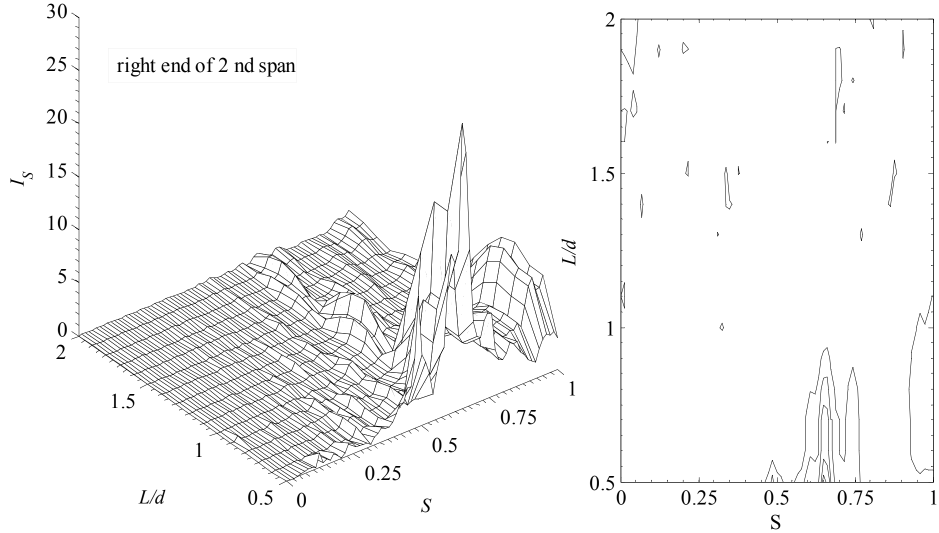

Figure 14. Effect o f the span to car length ratio on the impact factor for shear force at the right-end of second span: $I - S - L/d$ diagram and contour lines

6. CONCLUSIONS

In this study has been conducted to specify the effects of various parameters including the speed parameter and the span to car length ratio on the two-span bridge accelerations and impact factors. Dynamic responses and impact factors have been calculated for 16 bridges with different span lengths and 100 different velocities. The following conclusions can be drawn from the study:

1. The results show that an increase in the speed parameter causes an increase in the impact factor. If the operation speeds of the train can be controlled in the range with $0.0 \leq S < 0.4$ the minimal resonant responses will be induced on the bridge. On the other hand, smaller span to car length ratios lead to greater impact factor values.
2. Acceleration and impact factors for displacement, bending moment and shear force at any section of the first span are smaller than those for the second span.
3. Impact factors for shear force at the right-end of each span are smaller than those calculated at the left-end of each span.
4. When the span to car length ratio L/d equals 1.5, virtually no resonant responses for displacement, acceleration, bending moment and shear force will be induced on two-span bridges.

REFERENCES / KAYNAKLAR

[1] L.A. Frýba, Rough assessment of railway bridges for high speed trains, Engineering Structures, 23:548, 2001.
[2] J.D. Yau, Response of a train moving on multi-span railway bridges undergoing ground settlement, Engineering Structures, 31:2115, 2009.
[3] P. Museros, M.D. Martinez-Rodrigo, Vibration control of simply supported beams under moving loads using fluid viscous dampers, Journal of Sound and Vibration, 300:292, 2007.

[4] Y.B. Yang, J.D. Yau, L.C. Hsu, Vibration of simple beams due to trains moving at high speeds, Engineering Structures, 19:936, 1997.
[5] S.H. Ju, H.T. Lin, Resonance characteristics of high speed trains passing simply supported bridges, Journal of Sound and Vibration, 267:1127, 2003.
[6] J.D. Yau, J.D., Y.B. Yang, Vertical accelerations of simple beams due to successive loads traveling at resonant speeds, Journal of Sound and Vibration, 289:210, 2006.
[7] H. Xia, N. Zhang, W.W. Guo, Analysis of resonance mechanism and conditions of train-bridge system, Journal of Sound and Vibration, 297:810, 2006.
[8] R.S. Ayre, G. Ford, L.S. Jacobson, Transverse vibration of a two-span bridge under action of a moving constant force. Journal of Applied Mechanics, 17:1, 1950.
[9] K. Henchi, M. Fafard, Dynamic behavior of multi-span beams under moving loads, Journal of Sound and Vibration, 199:33, 1997.
[10] M. Ichikawa, A. Matsuda, Y. Miyakawa, Simple analysis of a multi-span beam under moving loads with variable velocity, Transactions of the Japan Society for Aeronautical and Spaces Sciences, 41:168, 1999.
[11] J.W. Kwark, E.S. Choi, Y.J. Kim, B.S. Kim, S.I. Kim, Dynamic behavior of two-span continuous concrete bridges under moving high-speed train, Computers and Structures, 82: 463, 2004.
[12] A.E. Martinez-Castro, P. Museros, A. Castillo-Linares, Semi-analytic solution in the time domain for non-uniform multi-span Bernoulli-Euler beams traversed by moving loads, Journal of Sound and Vibration, 294:278, 2006.
[13] C. Johansson, C. Pacoste, R. Karoumi, Closed-form solution for the mode superposition analysis of the vibration in multi-span beam bridges caused by concentrated moving loads, Computers and Structures, 119:85, 2013.
[14] S.A. Hamidi, F. Danshjoo, Determination of impact factor for steel railway bridges considering simultaneous effects of vehicle speed and axle distance to span length ratio, Engineering Structures, 32:1369, 2010.
[15] N.M. Newmark, A method of computation for structural dynamics, ASCE Journal of the Engineering Mechanics Division, 85:67, 1959.